Supplemental Material for "Active Jamming at Criticality"

Shalabh K. Anand,[1,2] Chiu Fan Lee,[1,*] and Thibault Bertrand[2,†]

[1] *Department of Bioengineering, Imperial College London, South Kensington Campus, London SW7 2AZ, U.K.*

[2] *Department of Mathematics, Imperial College London, South Kensington Campus, London SW7 2AZ, U.K.*

SCALING RELATION BETWEEN EXCESS COORDINATION AND PRESSURE

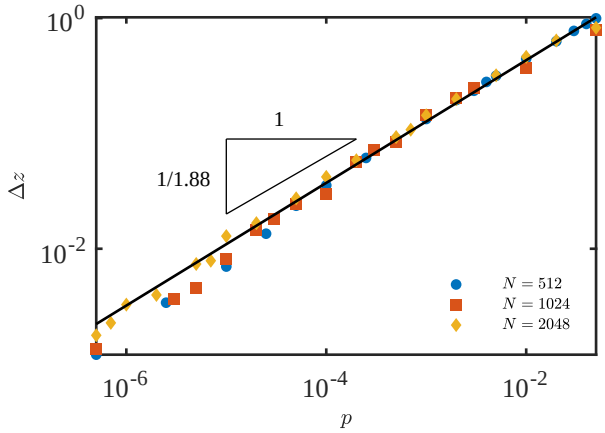


FIG. S1. Excess coordination Δz as a function of the pressure p. The solid line represents a power-law behavior with exponent 1/1.88.

Recently, Goodrich et al. [1] have argued that the excess coordination $\Delta z = z - z_{\rm iso}$ in static packings above the jamming threshold follows the following scaling relation with pressure

$$\Delta z \sim p^{1/1.88} \tag{S1}$$

Here, we confirm this scaling numerically by analyzing the static packings used as initial configurations for our numerical simulations. As presented in Fig. S1, Δz follows scaling relation (S1).

GAP DISTRIBUTION FOR STATIC PACKINGS

As argued in the main text, we expect the value of the critical active force to be dictated by the statistics of interparticle contacts in our overjammed static configurations. Those are in turn controlled by the distribution of gaps in static configurations at the jamming onset. As we overcompress our packings passed the jamming threshold, we expect gaps to close and new contacts to be formed. Conversely, as we increase the active force, we expect the particle coordination to decrease.

To show this, we compute the gap distribution for static packings of particles ($N = 2048$); we expect the gap distribution to follow a power-law behavior

$$P(h) \sim h^{-\gamma}. \tag{S2}$$

Figure S2 shows that the cumulative distribution of gaps $G(h) = \int_0^h P(h')dh'$ does indeed display a power-law behavior

$$G(h) \sim h^{1-\gamma} \tag{S3}$$

with scaling exponent $\gamma = 0.42 \pm 0.04$ measured for $p = 10^{-7}$. We note that the gap distribution is weakly dependent on the pressure p itself.

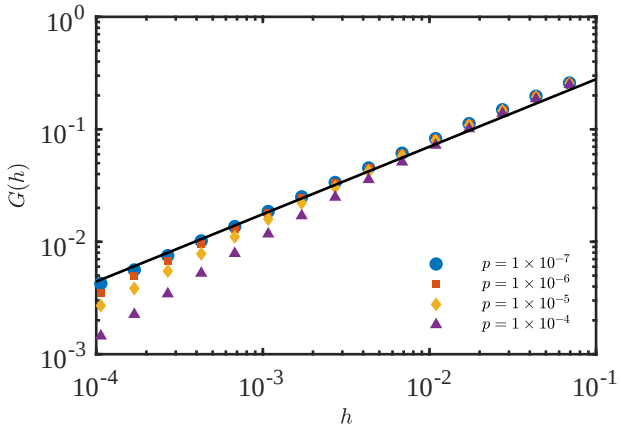


FIG. S2. Cumulative distribution of gaps between particles in static packings at various pressures $p \in [10^{-7}, 10^{-4}]$ for system size $N = 2048$.

EXCESS CONTACTS AS A FUNCTION OF ACTIVE FORCE

We estimate Δz for a series of active force strengths f for a given pressure p. We represent the surface formed by the excess coordination for all active force/pressure pairs in Fig. S3. We observe a monotonic decrease in excess coordination with active forces. The excess coordination eventually becomes zero (displayed by red line in Fig. S3).

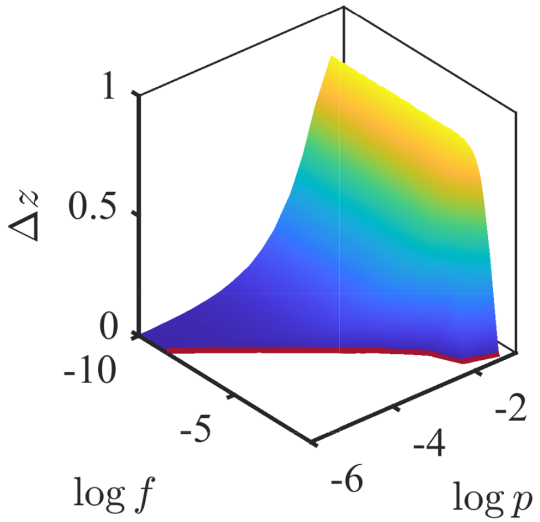


FIG. S3. Excess coordination Δz as a function of active force f and pressure p. The red line represents the strength of active force at which Δz becomes 0. The colormap indicates the magnitude of Δz.

SYSTEM SIZE EFFECT ON CRITICAL TEMPERATURE

In this section, we confirm the scaling of the critical temperature T_c with pressure p presented in Fig. 3 for a variety of system sizes from $N = 128$ to 4096. We show here that the critical temperature follows the same scaling with the pressure p for all system sizes tested (see Fig. S4), namely

$$f_{c,2} \equiv \sqrt{2T_c} \sim p^{3/2} \tag{S4}$$

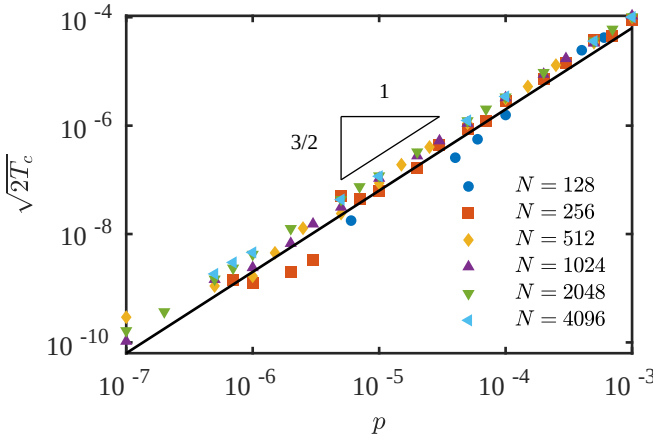


FIG. S4. System-size effect on the critical temperature T_c as a function of the pressure p.

DEVIATION FROM SCALING BEHAVIOR

To highlight the deviation from scaling behavior discussed in the main text, we here adopt a different representation of the data. For our ABPs simulations, we show below the rescaled critical active force $f_c/p^{3/2}$. In this representation, pure scaling behavior would manifest as a constant value of the rescaled critical active force as a function of pressure p. Any deviation from a constant value is a manifestation of a deviation from the scaling behavior. Here, we show that our ABPs simulations display a clear deviation from the scaling behavior observed in the vicinity of jamming onset at large values of the pressure p. As seen in Fig. S5, this representation further highlights that as the persistence of the active forcing decreases the regime of validity of the scaling behavior extends to higher pressure values.

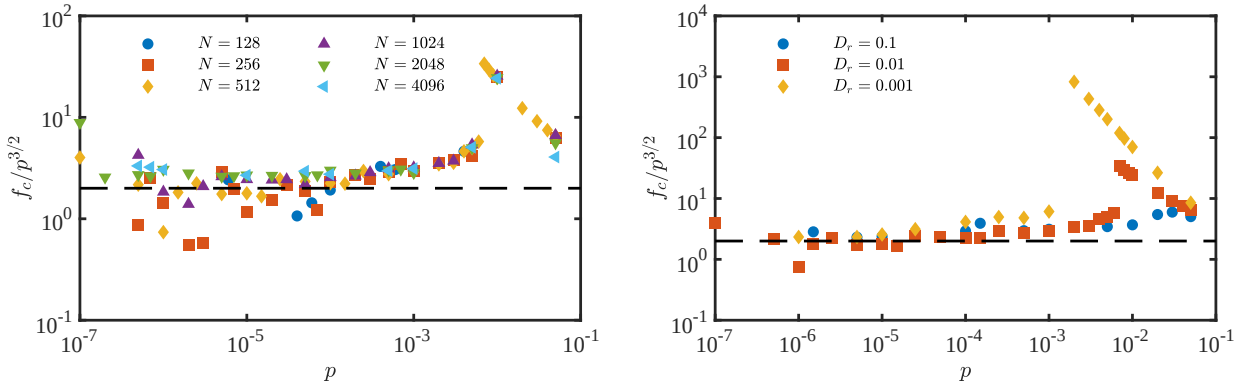


FIG. S5. *Scaling of the rescaled critical active force ($f_c/p^{3/2}$) vs. pressure (p) in active Brownian particles simulations.* (Left) Scaling behavior found for ABPs for various system sizes $N \in [128, 4096]$ consistent with a power-law scaling with exponent $\chi = 3/2$ (dashed black line). In this representation, the deviation from the scaling behavior observed in the vicinity of the jamming onset is highlighted at large pressure values. (Right) Scaling behavior observed for ABPs with various persistence D_r^{-1} and $N = 512$. Once again, in this representation we have highlighted the deviation from scaling behavior at large pressure values; this clearly shows that as the persistence of the active forcing decreases the regime of validity of the scaling behavior extends to higher pressure values.

DYNAMICAL SIGNATURES OF UNJAMMING

Here, we concluded to the existence of a finite-sized active jammed region in the vicinity of the athermal jamming point. To reach this conclusion, we defined jammed states as those possessing a positive steady-state time-averaged excess coordination. This is a natural extension of the jammed states definition used in the athermal passive case. Nevertheless, in this section, we exhibit three dynamical quantities of interest which display clear signatures of this

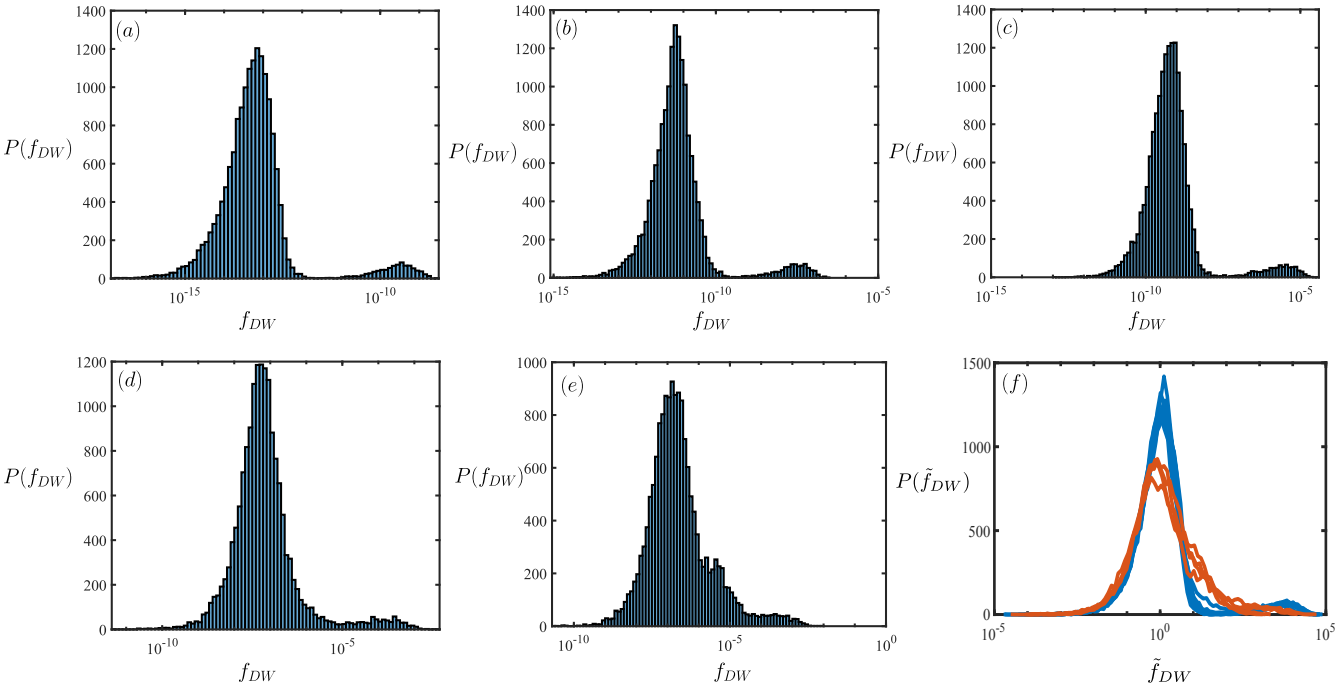


FIG. S6. Distribution of Debye-Waller (DW) factor for systems initially at pressure $p = 10^{-4}$ for strength of active forces both below and above the critical active force f_c. Active force magnitudes are given as follows (a) $f = 10^{-9}$, (b) $f = 10^{-8}$, (c) $f = 10^{-7}$, (d) $f = 2 \times 10^{-6}$ and (e) $f = 3 \times 10^{-6}$. At pressure $p = 10^{-4}$, the critical active force is measured to be $f_c = 2.24 \times 10^{-6}$. (f) Distribution of rescaled and shifted DW factors $\tilde{f}_{\rm DW}$. Blue lines denote distributions with $f < f_c$ exhibiting a clearly bimodal distribution characteristic of a mechanically stable vibrating backbone accompanied by floaters while orange lines denote distributions for $f > f_c$ for which bimodality has disappeared.

critical transition.

To characterize the dynamics of our systems, we focus first on single particle dynamics. A first correlation function to study is the mean-squared displacement (MSD); from our simulations, it is easily measured as

$$\Delta^2(t) = \frac{1}{N}\sum_{i=1}^{N}\langle|\Delta\mathbf{r}_i(t)|^2\rangle \tag{S5}$$

where $\Delta\mathbf{r}_i(t) = \mathbf{r}_i(t) - \mathbf{r}_i(0)$ and $\mathbf{r}_i(t)$ represents the time-dependent position of particle i. Note that the brackets in Eq. (S5) represent an average over long-time trajectories. The long-time limit of the MSD is commonly called the Debye-Waller (DW) factor.

The measure of the MSD for jammed packings is notoriously plagued by the dynamics of so-called floaters. Floaters are a small fraction of particles from the original packing which are not part of the mechanically stable backbone of the static packing. Being less connected than other particles, floaters have peculiar dynamical properties. In particular, when the systems is subject to thermal or active fluctuations, they move much more than the other particles and so their dynamics, while not representative of the overall dynamics of the system, may dominate the sum in Eq. (S5).

One way to deal with floaters is to remove them from the sum in Eq. (S5); to do so, we need to identify the floaters which is not an easy task in a dynamic packing. In an overcompressed static packing, floaters are identified based on force balance considerations. Namely, they are defined as particles having strictly less than 3 contacts and easily removed recursively. However, this method can not be used for either unjammed states or dynamical states (as particles may come in and out of contact). Instead, our definition of floaters follows from [2] where floaters are defined as particles whose DW factor $f_{\rm DW}$ is 5 times larger than the median DW factor $\bar{f}_{\rm DW}$. Once identified, the N_f floaters are removed from the sum in Eq. (S5) which thus runs to $N' = N - N_f$.

The distributions of observed DW factors $P(f_{\rm DW})$ in configurations subject to active forces is very informative. As seen in Fig. S6, static packings at pressure $p = 10^{-4}$ subject to active forces below the critical active forces display a bimodal DW factor distributions [see Fig. S6(a)-(c)]. In these bimodal distributions, the peak at higher DW factors is much smaller in amplitude and is a clear signature of the floaters. As the driving active force is increased above the

critical active force measured via the excess coordination, we observe a merging of the two peaks in the distribution which becomes unimodal [see Fig. S6(d)-(e)]. This is clear in Fig. S6(f) where we represent the distribution of rescaled DW factors $\tilde{f}_{\mathrm{DW}} = f_{\mathrm{DW}}/\bar{f}_{\mathrm{DW}}$, where $\bar{f}_{DW}$ denotes the median of the distribution.

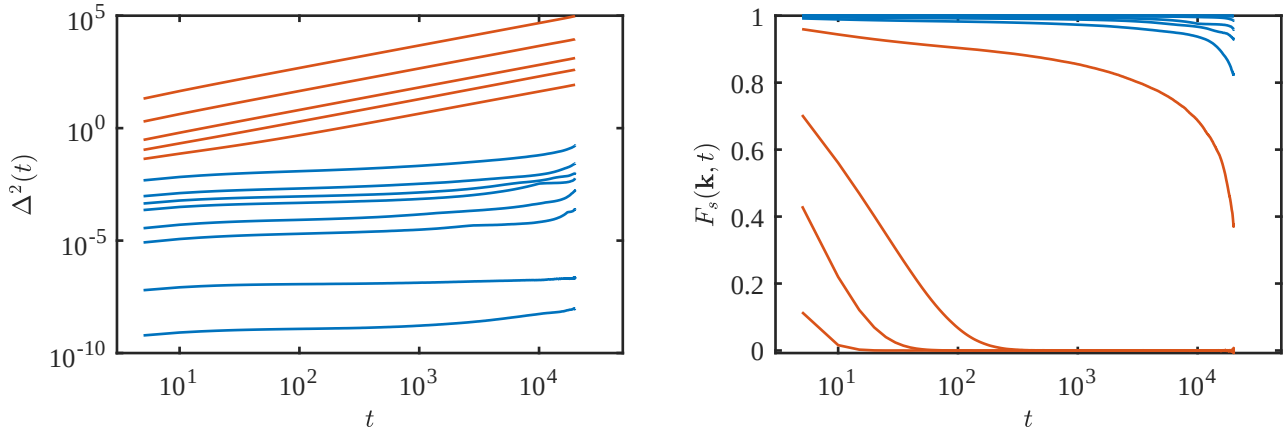


FIG. S7. (a) Mean-squared displacement $\Delta^2(t)$ and (b) self intermediate scattering function $F_s(\mathbf{k},t)$ measured in systems initially at pressure $p = 10^{-2}$ and subject to active forces below and above the critical active force $f_c = 0.0245$. As in Fig. S6, color encodes the value of the active forces relative to the critical active force.

Armed with a definition for the floaters, we can now compute unambiguously the mean-squared displacement $\Delta^2(t)$ for systems subjected to active forces below and above the critical active force. Fig. S7(a) shows that for all active forces $f < f_c$, the MSD clearly plateaus and our packings are fully caged (over the timescale of our long-time simulations). For $f > f_c$, we observe a strikingly different behavior with diffusive MSDs and we conclude that the system is unjammed passed the critical active force f_c. Finally, we compute the self intermediate scattering function (ISF) over the same simulations. The ISF is defined as

$$F_s(\mathbf{k},t) = \frac{1}{N}\left\langle \sum_{i=1}^{N'} \exp\left[\imath\mathbf{k}\cdot(\mathbf{r}_i(t) - \mathbf{r}_i(0))\right]\right\rangle \tag{S6}$$

where the wave vector $\mathbf{k}$ was chosen to be proportional to the inverse of the position of the first peak in the radial pair correlation function $g(r)$. Fig. S7 shows clearly that the ISF does not significantly decay over the full timescale of our simulations when $f < f_c$; we thus conclude to the lack of structural rearrangements over the course of these simulations. On the other hand, for $f > f_c$, we observe a very fast and sharp decay of the ISF to zero clearly denoting unjammed states. Altogether, these observations support our choice of excess coordination as a key parameter to identify the critical strength of active force for the transition.

* c.lee@imperial.ac.uk
† t.bertrand@imperial.ac.uk

[1] C. P. Goodrich, A. J. Liu, and J. P. Sethna, "Scaling ansatz for the jamming transition," Proceedings of the National Academy of Sciences **113**, 9745–9750 (2016).
[2] A. Ikeda, L. Berthier, and G. Biroli, "Dynamic criticality at the jamming transition," The Journal of Chemical Physics **138**, 12A507 (2013).